Novel R tools for analysis of genome-wide population genetic data with emphasis on clonality

Zhian N. Kamvar [1]**, Jonah C. Brooks** [2]**, Niklaus J. Grünwald** [1,3*]

[1] *Botany and Plant Pathology, Oregon State University, Corvallis, OR, USA*

[2] *College of Electrical Engineering and Computer Science, Oregon State University, Corvallis, OR, USA*

[3] *Horticultural Crops Research Laboratory, USDA-Agricultural Research Service, Corvallis, OR, USA*

Correspondence*:
Niklaus J. Grünwald
Horticultural Crops Research Laboratory USDA ARS
3420 NW Orchard Ave.
Corvallis, OR, 97330, `grunwaln@science.oregonstate.edu`

ABSTRACT

To gain a detailed understanding of how plant microbes evolve and adapt to hosts, pesticides, and other factors, knowledge of the population dynamics and evolutionary history of populations is crucial. Plant pathogen populations are often clonal or partially clonal which requires different analytical tools. With the advent of high throughput sequencing technologies, obtaining genome-wide population genetic data has become easier than ever before. We previously contributed the R package *poppr* specifically addressing issues with analysis of clonal populations. In this paper we provide several significant extensions to *poppr* with a focus on large, genome-wide SNP data. Specifically, we provide several new functionalities including the new function `mlg.filter` to define clone boundaries allowing for inspection and definition of what is a clonal lineage, a sliding-window analysis of the index of association, modular bootstrapping of any genetic distance, and analyses across any level of hierarchies.

Keywords: clonality, population genomics, bootstrap, index of association, hierarchical analysis, sliding window

INTRODUCTION

To paraphrase Dobzhansky, nothing in the field of plant-microbe interactions makes sense except in the light of population genetics (Dobzhansky, 1973). Genetic forces such as selection and drift act on alleles in a population. Thus, a true understanding of how plant pathogens emerge, evolve and adapt to crops, fungicides, or other factors, can only be elucidated in the context of population level phenomena given the demographic history of populations (McDonald and Linde, 2002; Grünwald and Goss, 2011; Milgroom et al., 1989). The field of population genetics, in the era of whole genome resequencing, provides unprecedented power to describe the evolutionary history and population processes that drive coevolution between pathogens and hosts. This powerful field thus critically enables effective deployment of R genes, design of pathogen informed plant resistance breeding programs, and implementation of fungicide rotations that minimize emergence of resistance.

Most computational tools for population genetics are based on concepts developed for sexual model organisms. Populations that reproduce clonally or are polyploid are thus difficult to characterize using

27   classical population genetic tools because theoretical assumptions underlying the theory are violated. Yet,
28   many plant pathogen populations are at least partially clonal if not completely clonal (Milgroom, 1996;
29   Anderson and Kohn, 1995). Thus, development of tools for analysis of clonal or polyploid populations is
30   needed.

31   Genotyping by sequencing and whole genome resequencing provide the unprecedented ability to
32   identify thousands of single nucleotide polymorphisms (SNPs) in populations (Elshire et al., 2011; Luikart
33   et al., 2003; Davey et al., 2011). With traditional marker data (e.g., SSR, AFLP) a clone was typically
34   defined as a unique multilocus genotype (MLG) (Grünwald and Hoheisel, 2006; Falush et al., 2003; Goss
35   et al., 2009; Cooke et al., 2012; Taylor and Fisher, 2003). Availability of large SNP data sets provides new
36   challenges for data analysis. These data are based on reduced representation libraries and high throughput
37   sequencing with moderate sequencing depth which invariably results in substantial missing data, error in
38   SNP calling due to sequencing error, lack of read depth or other sources of spurious allele calls (Mastretta-
39   Yanes et al., 2015). It is thus not clear what a clone is in large SNP data sets and novel tools are required
40   for definition of clone boundaries.

41   The research community using the R statistical and computing language (R Core Team, 2015) has
42   developed a plethora of new resources for population genetic analysis (Paradis, 2010; Jombart, 2008).
43   R is particularly appealing because all code is open source and functions can be evaluated and modified
44   by any user. Recently, we introduced the R package *poppr* specifically developed for analysis of clonal
45   populations (Kamvar et al., 2014b). *Poppr* previously introduced several novel features including the
46   ability to conduct a hierarchical analysis across unlimited hierarchies, test for linkage association, graph
47   minimum spanning networks or provide bootstrap support for Bruvo's distance in resulting trees. *Poppr*
48   has been rapidly adopted and applied to a range of studies including for example horizontal transmission
49   in leukemia of clams (Metzger et al., 2015), study of the vector-mediated parent-to-offspring transmission
50   in an avian malaria-like parasite (Chakarov et al., 2015), and characterization of the emergence of the
51   invasive forest pathogen *Hymenoscyphus pseudoalbidus* (Gross et al., 2014). It has also been used to
52   implement real-time, online shinyR based tools for visualizing relationships among unknown MLGs in
53   reference databases (http ://phytophthora-id.org/) (Grünwald et al., 2011).

54   Here, we introduce *poppr* 2.0, which provides a major update to *poppr* (Kamvar et al., 2014b) including
55   novel tools for analysis of clonal populations specifically addressing large SNP data. Significant novel
56   tools include functions for calculating clone boundaries and collapsing individuals into clonal groups
57   based on a user-specified genetic distance threshold, sliding window analyses, genotype accumulation
58   curves, reticulations in minimum spanning networks, and bootstrapping for any genetic distance.

IMPLEMENTATIONS AND EXAMPLES

CLONAL IDENTIFICATION

59   As highlighted in previous work, clone correction is an important component of population genetic
60   analysis of organisms that are known to reproduce asexually (Kamvar et al., 2014b; Milgroom, 1996;
61   Grünwald et al., 2003). This method is a partial correction for bias that affects metrics that rely on allele
62   frequencies assuming panmixia. It was initially designed for data with only a handful of markers. With the
63   advent of large-scale sequencing and reduced- representation libraries, it has become easier to sequence
64   tens of thousands of markers from hundreds of individuals (Elshire et al., 2011; Davey et al., 2011; Davey
65   and Blaxter, 2010). With this larger number of markers, the genetic resolution is much greater, but the
66   chance of genotyping error is also greatly increased and missing data is frequent (Mastretta-Yanes et al.,
67   2015). Taking this fact and occasional somatic mutations into account, it would be impossible to separate
68   true clones from independent individuals by just comparing what MLGs are different. We introduce a
69   new method for collapsing unique multilocus genotypes determined by naive string comparison into
70   multilocus lineages utilizing any genetic distance given three different clustering algorithms: farthest
71   neighbor, nearest neighbor, and UPGMA (average neighbor) (Sokal, 1958).

72   These clustering algorithms act on a distance matrix that is either provided by the user or generated via
73 a function that will calculate a distance from genclone objects such as `bruvo.dist`, which in particular
74 applies to any level of ploidy (Bruvo et al., 2004). All algorithms have been implemented in C and
75 utilize the OpenMP framework for optional parallel processing (Dagum and Menon, 1998). Default is the
76 conservative farthest neighbor algorithm (Fig. 1A), which will only cluster samples together if all samples
77 in the cluster are at a distance less than the given threshold. By contrast, the nearest neighbor algorithm
78 will have a chaining effect that will cluster samples akin to adding links on a chain where a sample can
79 be included in a cluster if all of the samples have at least one connection below a given threshold (Fig.
80 1C). The UPGMA, or average neighbor clustering algorithm is the one most familiar to biologists as it is
81 often used to generate ultra-metric trees based on genetic distance (Fig. 1B). This algorithm will cluster by
82 creating a representative sample per cluster and joining clusters if these representative samples are closer
83 than the given threshold.

84   We utilize data from the microbe *Phytophthora infestans* to show how the `mlg.filter` function
85 collapses multilocus genotypes with Bruvo's distance assuming a genome addition model (Bruvo et
86 al., 2004). *P. infestans* is the causal agent of potato late blight originating from Mexico that spread to
87 Europe in the mid 19th century (Goss et al., 2014; Yoshida et al., 2013). *P. infestans* reproduces both
88 clonally and sexually. The clonal lineages of *P. infestans* have been formally defined into 18 separate
89 clonal lineages using a combination of various molecular methods including AFLP and microsatellite
90 markers (Lees et al., 2006; Li et al., 2013). For these data, we used `mlg.filter` to detect all of the
91 distance thresholds at which 18 multilocus lineages would be resolved. We used these thresholds to define
92 multilocus lineages and create contingency tables and dendrograms to determine how well the multilocus
93 lineages were detected.

94   For the *P. infestans* population, the three algorithms were able to detect 18 multilocus lineages at
95 different distance thresholds (Fig. 2). Contingency tables between the described multilocus genotypes
96 and the genotypes defined by distance show that most of the 18 lineages were resolved, except for US-8,
97 which is polytomic (Table 1).

98   We utilized simulated data to evaluate the effect of sequencing error and missing data on MLG calling.
99 We constructed the data using the `glSim` function in *adegenet* (Jombart and Ahmed, 2011) to obtain a
100 SNP data set for demonstration. Two diploid data sets were created, each with 10k SNPs (25% structured
101 into two groups) and 200 samples with 10 ancestral populations of even sizes. Clones were created in one
102 data set by marking each sample with a unique identifier and then randomly sampling with replacement.
103 It is well documented that reduced- representation sequencing can introduce several erroneous calls and
104 missing data (Mastretta-Yanes et al., 2015). To reflect this, we mutated SNPs at a rate of 10% and inserted
105 an average of 10% missing data for each sample after clones were created, ensuring that no two sequences
106 were alike. The number of mutations and missing data per sample were determined by sampling from
107 a Poisson distribution with $\lambda = 1000$. After pooling, 20% of the data set was randomly sampled for
108 analysis. Genetic distance was obtained with the function `bitwise.dist`, which calculates the fraction
109 of different sites between samples equivalent to Provesti's distance, counting missing data as equivalent
110 in comparison (Prevosti et al., 1975).

111   All three filtering algorithms were run with a threshold of 1, returning a numeric vector of length $n - 1$
112 where each element represented a threshold at which two samples/clusters would join. Since each data set
113 would have varying distances between samples, the clonal boundary threshold was defined as the midpoint
114 of the largest gap between two thresholds that collapsed less than 50% of the data.

115   Out of the 100 simulations run, we found that across all methods, detection of duplicated samples had
116 $\sim$ 98% true positive fraction and $\sim$ 0.8% false positive fraction indicating that this method is robust to
117 simulated populations.

MINIMUM SPANNING NETWORKS WITH RETICULATION

118 In its original iteration, *poppr* introduced minimum spanning networks that were based on the *igraph*
119 function `minimum.spanning.tree` (Csardi and Nepusz, 2006). This algorithm produces a minimum
120 spanning tree with no reticulations where nodes represent individual MLGs. In other minimum spanning
121 network programs, reticulation is obtained by calculating the minimum spanning tree several times and
122 returning the set of all edges included in the trees. Due to the way *igraph* has implemented Prim's
123 algorithm, it is not possible to utilize this strategy, thus we implemented an internal C function to walk
124 the space of minimum spanning trees based on genetic distance to connect groups of nodes with edges of
125 equal weight.

126 To demonstrate the utility of minimum spanning networks with reticulation, we used two clonal data
127 sets: the H3N2 flu virus data from the *adegenet* package using years of each epidemic as the population
128 factor, and *Phytophthora ramorum* data from Nurseries and Oregon forests (Jombart et al., 2010; Kamvar
129 et al., 2014a). Minimum spanning networks were created with and without reticulation using the *poppr*
130 functions `diss.dist` and `bruvo.msn` for the H3N2 and *P. ramorum* data, respectively (Kamvar et
131 al., 2014b; Bruvo et al., 2004). To detect mlg clusters, the infoMAP community detection algorithm was
132 applied with 10,000 trials as implemented in the R package *igraph* version 0.7.1 utilizing genetic distance
133 as edge weights and number of samples in each MLG as vertex weights (Csardi and Nepusz, 2006; Rosvall
134 and Bergstrom, 2008).

135 To evaluate the results, we compared the number, size, and entropy (H) of the resulting communities
136 as we expect a highly clonal organism with low genetic diversity to result in a few, large communities.
137 We also created contingency tables of the community assignments with the defined populations and used
138 those to calculate entropy using Shannon's index with the function `diversity` from the R package
139 *vegan* version 2.2-1 (Oksanen et al., 2015; Shannon, 2001). A low entropy indicates presence of a few
140 large communities whereas high entropy indicates presence of many small communities.

141 The infoMAP algorithm revealed 63 communities with a maximum community size of 77 and $H = 3.56$
142 for the reticulate network of the H3N2 data and 117 communities with a maximum community size of
143 26 and $H = 4.65$ for the minimum spanning tree. The entropy across years was greatly decreased for
144 all populations with the reticulate network compared to the minimum spanning tree (Fig. 3). Note that
145 the reticulated network (Fig. 3B) showed patterns corresponding with those resulting from a discriminant
146 analysis of principal components (Fig. 3D) (Jombart et al., 2010).

147 Graph walking of the reticulated minimum spanning network of *P. ramorum* by the infoMAP algorithm
148 revealed 16 communities with a maximum community size of 13 and $H = 2.60$. The un-reticulated
149 minimum spanning tree revealed 20 communities with a maximum community size of 7 and $H = 2.96$.
150 In the ability to predict Hunter Creek as belonging to a single community, the reticulated network was
151 successful whereas the minimum spanning tree separated one genotype from that community. The entropy
152 for the reticulated network was lower for all populations except for the coast population (supplementary
153 information).

BOOTSTRAPPING

154 Assessing population differentiation through methods such as G_{st}, AMOVA, and Mantel tests relies on
155 comparing samples within and across populations (Nei, 1973; Excoffier et al., 1992; Mantel, 1967).
156 Confidence in distance metrics is related to the confidence in the markers to accurately represent the
157 diversity of the data. Especially true with microsatellite markers, a single hyper-diverse locus can make a
158 population appear to have more diversity based on genetic distance. Using a bootstrapping procedure of
159 randomly sampling loci with replacement when calculating a distance matrix provides support for clades
160 in hierarchical clustering.

161 Data in genind and genpop objects are represented as matrices with individuals in rows and alleles in
162 columns (Jombart, 2008). This gives the advantage of being able to use R's matrix algebra capabilities

163 to efficiently calculate genetic distance. Unfortunately, this also means that bootstrapping is a non- trivial
164 task as all alleles at a single locus need to be sampled together. To remedy this, we have created an internal
165 S4 class called "bootgen", which extends the internal "gen" class from *adegenet*. This class can be created
166 from any genind, genclone, or genpop object, and allows loci to be sampled with replacement. To further
167 facilitate bootstrapping, a function called `aboot`, which stands for "any boot", is introduced that will
168 bootstrap any genclone, genind, or genpop object with any genetic distance that can be calculated from it.

169   To demonstrate calculating a dendrogram with bootstrap support, we used the *poppr* function `aboot`
170 on population allelic frequencies derived from the data set `microbov` in the *adegenet* package with
171 1000 bootstrap replicates (Jombart, 2008; Laloë et al., 2007). The resulting dendrogram shows bootstrap
172 support values $> 50\%$ (Fig. 4) and used the following code:

```
library("poppr")
data("microbov", package = "adegenet")
strata(microbov) <- data.frame(other(microbov))
setPop(microbov) <- ~coun/spe/breed
bov_pop <- genind2genpop(microbov)

set.seed(20150428)
pop_tree <- aboot(bov_pop, sample = 1000, cutoff = 50)
```

GENOTYPE ACCUMULATION CURVE

173 Analysis of population genetics of clonal organisms often borrows from ecological methods such as
174 analysis of diversity within populations (Milgroom, 1996; Arnaud-Hanod et al., 2007; Grünwald et al.,
175 2003). When choosing markers for analysis, it is important to make sure that the observed diversity in your
176 sample will not appreciably increase if an additional marker is added (Arnaud-Hanod et al., 2007). This
177 concept is analogous to a species accumulation curve, obtained by rarefaction. The genotype accumulation
178 curve in *poppr* is implemented in the function `genotype_curve`. The curve is constructed by randomly
179 sampling x loci and counting the number of observed MLGs. This repeated r times for 1 locus up to $n - 1$
180 loci, creating $n - 1$ distributions of observed MLGs.

181   The following code example demonstrates the genotype accumulation curve for data from Everhart and
182 Scherm (2015) showing that these data reach a small plateau and have a greatly decreased variance with
183 12 markers, indicating that there are enough markers such that adding more markers to the analysis will
184 not create very many new genotypes (Fig. 5).

```
library("poppr")
library("ggplot2")
data("monpop", package = "poppr")

set.seed(20150428)
genotype_curve(monpop, sample = 1000)
p <- last_plot() + theme_bw()   # get the last plot
p + geom_smooth(aes(group = 1)) # plot with a trendline
```

INDEX OF ASSOCIATION

185 The index of association (I_A) is a measure of multilocus linkage disequilibrium that is most often used
186 to detect clonal reproduction within organisms that have the ability to reproduce via sexual or asexual
187 processes (Brown et al., 1980; Smith et al., 1993; Milgroom, 1996). It was standardized in 2001 as
188 $\bar{r}_d$ by Agapow and Burt (2001) to address the issue of scaling with increasing number of loci. This
189 metric is typically applied to traditional dominant and co-dominant markers such as AFLPs, SNPs, or

190 microsatellite markers. With the advent of high throughput sequencing, SNP data is now available in a
191 genome-wide context and in very large matrices including thousands of SNPs. For this reason, we devised
192 two approaches using the index of association for large numbers of markers typical for population genomic
193 studies. Both functions utilize *adegenet*'s "genlight" object class, which efficiently stores 8 binary alleles
194 in a single byte (Jombart and Ahmed, 2011). As calculation of the $\bar{r}_d$ requires distance matrices of absolute
195 number of differences, we utilize a function that calculates these distances directly from the compressed
196 data called `bitwise.dist`.

197   The first approach is a sliding window analysis implemented in the function `win.ia`. It utilizes the
198 position of markers in the genome to calculate $\bar{r}_d$ among any number of SNPs found within a user-
199 specified windowed region. It is important that this calculation utilize $\bar{r}_d$ as the number of loci will be
200 different within each window (Agapow and Burt, 2001). This approach would be suited for a quick
201 calculation of linkage disequilibrium across the genome that can detect potential hotspots of LD that
202 could be investigated further with more computationally intensive methods assuming that the number of
203 samples $<<$ the number of loci.

204   As it would necessarily focus on loci within a short section of the genome that may or may not
205 be recombining, a sliding window approach would not be good for utilizing $\bar{r}_d$ as a test for clonal
206 reproduction. A remedy for this is implemented in the function `samp.ia`, which will randomly sample
207 m loci, calculate $\bar{r}_d$, and repeat r times, thus creating a distribution of expected values of $\bar{r}_d$.

208   To demonstrate the sliding window and random sampling of $\bar{r}_d$ with respect to clonal populations, we
209 simulated two populations containing 1,100 neutral SNPs for 100 diploid individuals under the same
210 initial seed. One population had individuals randomly sampled with replacement, representing the clonal
211 population. After sampling, both populations had 5% random error and 1% missing data independently
212 propagated across all samples. On average, we obtained a higher value of $\bar{r}_d$ for the clonal population
213 compared to the sexual population for both methods (Fig. 6).

DATA FORMAT UPDATES: POPULATION STRATA AND HIERARCHIES

214 Assessments of population structure through methods such as hierarchical F_{st} (Goudet, 2005) and
215 AMOVA (Michalakis and Excoffier, 1996) require hierarchical sampling of populations across space
216 or time (Linde et al., 2002; Everhart and Scherm, 2015; Grünwald and Hoheisel, 2006). With clonal
217 organisms, basic practice has been to clone-censor data to avoid downward bias in diversity due to
218 duplicated genotypes that may or may not represent different samples (Milgroom, 1996). This correction
219 should be performed with respect to a population hierarchy to accurately reflect the biology of the
220 organism. Traditional data structures for population genetic data in most analysis tools allow for only
221 one level of hierarchical definition. The investigator thus had to provide the data set for analysis at each
222 hierarchical level.

223   To facilitate handling hierarchical and mutlilocus genotypic metadata, *poppr* version 1.1 introduced
224 a new S4 data object called "genclone", extending *adegenet*'s "genind" object (Kamvar and Grünwald,
225 unpublished). The genclone object formalized the definitions of multilocus genotypes and population
226 hierarchies by adding two slots called "mlg" and "hierarchy" that carried a numeric vector and a data
227 frame, respectively. These new slots allow for increased efficiency and ease of use by allowing these
228 metadata to travel with the genetic data. The hierarchy slot in particular contains a data frame where each
229 column represents a separate hierarchical level. This is then used to set the population factor of the data by
230 supplying a hierarchical formula containing one or more column names of the data frame in the hierarchy
231 slot.

232   The functionality represented by the hierarchy slot has now been migrated from the *poppr* to the
233 *adegenet* package version 2.0 to allow hierarchical analysis in *adegenet*, *poppr*, and other dependent
234 packages. The prior *poppr* `hierarchy` slot and methods have now been renamed `strata` in *adegenet*.
235 A short example of the utility of these methods can be seen in the code segment under **Bootstrapping**,

236 above. This migration provides end users with a broader ability to analyze data hierarchically in R across
237 packages.

AVAILABILITY

238 As of this writing, the *poppr* R package version 2.0 containing all of the features described here
239 is located at `https://github.com/grunwaldlab/poppr/tree/2.0-rc`. It is necessary
240 to install *adegenet* 2.0 before installing *poppr*. It can be found at `https://github.com/`
241 `thibautjombart/adegenet`. Both of these can be installed via the R package *devtools* (Wickham
242 and Chang, 2015):

```
library("devtools")
install_github("thibautjombart/adegenet")
install_github("grunwaldlab/poppr@2.0-rc")
```

243 Several population genetics packages in R are currently going through a major upgrade
244 following the 2015 R hackathon on population genetics (`https://github.com/NESCent/`
245 `r-popgen-hackathon`) and have not yet been updated in CRAN. We will upload *poppr* 2.0 to CRAN
246 once all other reverse dependent packages have been updated.

DISCUSSION

247 Given low cost and high throughput of current sequencing technologies we are entering a new era of
248 population genomics where large SNP data sets with thousands of markers are becoming available for
249 large populations in an genome-wide context. This data provides new possibilities and challenges for
250 population genetic analyses. We provide novel tools that enable analysis of this data in R with a particular
251 emphasis on clonal organisms.

252 Particularly useful is the implementation of $\bar{r}_d$ in a genomic context (Agapow and Burt, 2001). Random
253 sampling of loci across the genome can give an expected distribution of $\bar{r}_d$, which is expected to have
254 a mean of zero for panmictic populations. This metric is not affected by the number of loci sampled, is
255 model free, and has the ability to detect population structure. $\bar{r}_d$ is also implemented for sliding window
256 analyses that are useful to detect candidate regions of linkage disequilibrium for further analysis.

257 Clustering multilocus genotypes into multilocus lineages based on genetic distances is a non-trivial
258 task given large SNP data sets. Moreover, this has not previously been implemented for genomic data
259 for clonal populations. Clonal assignment has previously been available in the programs GENCLONE
260 and GENODIVE (Arnaud-Hanod et al., 2007; Meirmans and Van Tienderen, 2004). Our method with
261 `mlg.filter` builds upon this idea and allows the user to choose between three different approaches
262 for clustering MLGs. As diagrammed in Fig. 1 and demonstrated in Fig. 2, it is clear that the choice of
263 clustering algorithm has an impact on the data, where for example a genetic distance cutoff of 0.1 would
264 be the difference between 14 multilocus lineages (MLLs) and 17 MLLs for nearest neighbor and UPGMA
265 clustering, respectively (Fig. 2). The option to choose the clustering algorithm gives the user the ability
266 to choose what is biologically relevant to their populations. While there is not one optimal procedure for
267 defining boundaries in clonal lineages, our tool provides a means of exploring the potential MLG or MLL
268 boundary space.

269 Reticulation of minimum spanning networks provides improved ability to resolve relationships,
270 particularly for clonal populations. For clonal organisms, reticulate minimum spanning networks can
271 be thought off as a chain, implying that the clones are derived in a progressive and linear fashion by
272 accumulation of mutations within a clone. The current implementation in *poppr* has been successfully
273 used in analyses such as reconstruction of the *P. ramorum* epidemic in Oregon forests (Kamvar et al.,

274 2014a, 2015). Reticulated networks allow for the application of graph community detection algorithms
275 such as the infoMAP algorithm (Rosvall and Bergstrom, 2008).

276   *Popper* 2.0 is open source and available on github. Members of the community are invited to contribute
277 by raising issues or pull requests on our repository at `https://github.com/grunwaldlab/`
278 `poppr/issues`.

ACKNOWLEDGEMENTS

FIGURES AND TABLES

FIGURE 1

FIGURE 2

P. infestans reference isolates (12 SSR loci)

FIGURE 3

288

FIGURE 4

289

FIGURE 5

290

FIGURE 6

291
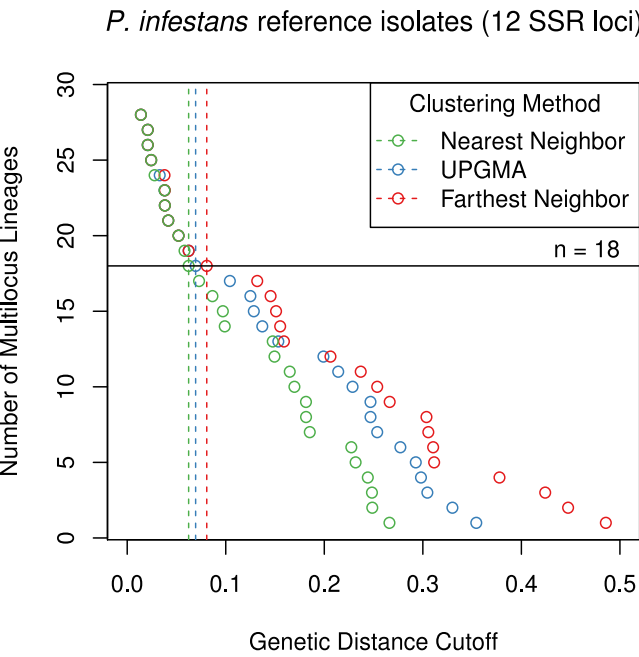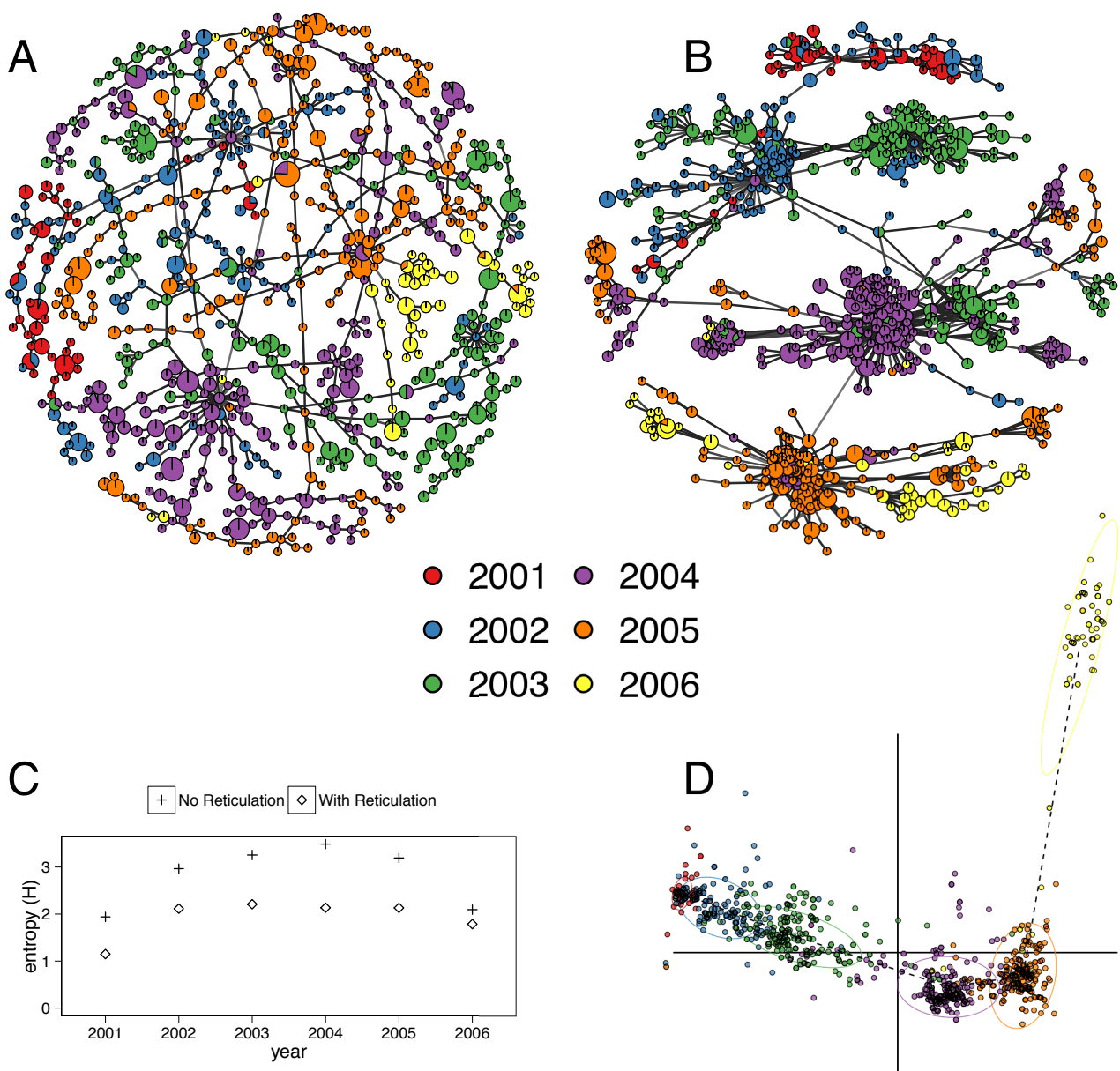
292   **Table 1** Contingency table comparing multilocus lineages assigned based on average neighbor clustering
293   (columns) vs. multilocus lineages defined in Li et al. (2013) and Lees et al. (2006).

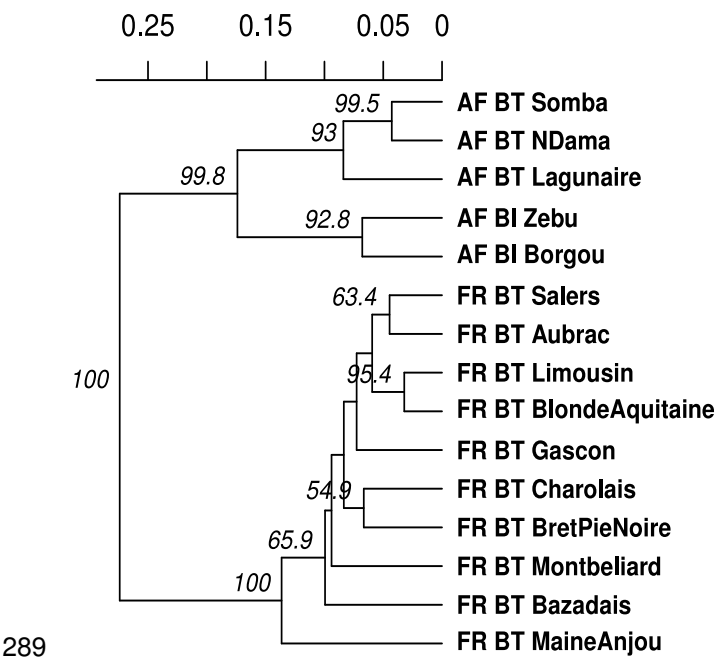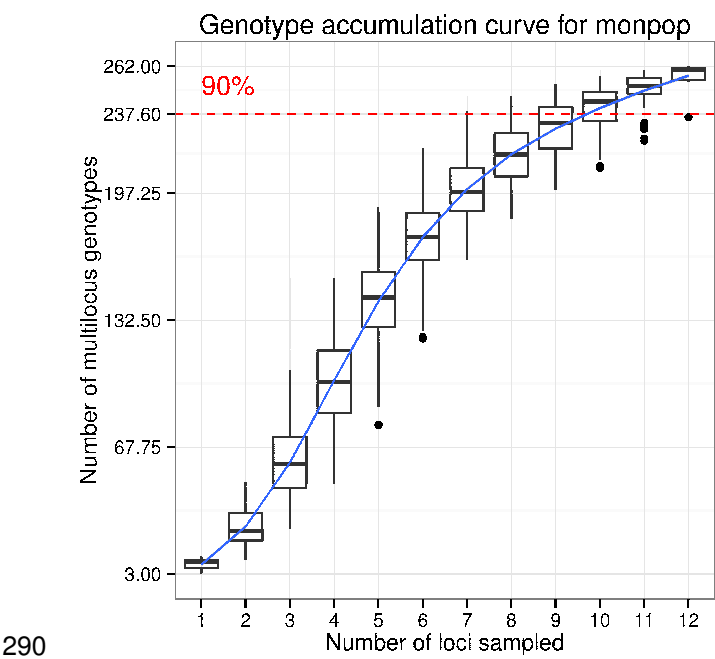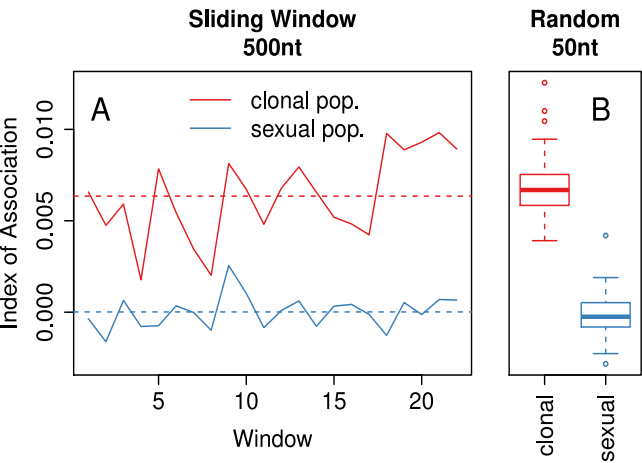|	3	4	5	6	8	10	12	15	16	17	18	20	21	22	24	25	27	28
B	.	.	.	.	.	.	.	.	.	.	.	.	.	.	.	1	.	.
C	.	.	.	.	.	.	.	.	.	.	.	.	.	.	1	.	.	.
D.1	.	.	.	.	.	.	.	.	.	.	.	.	.	1	.	.	.	.
D.2	.	.	.	.	.	.	.	1	.	.	.	.	.	1	.	.	.	.
EU-13	.	.	.	.	.	.	.	.	1	.	.	.	.	.	.	.	.	.
EU-4	.	.	.	.	.	.	.	.	.	1	.	.	.	.	.	.	.	.
EU-5	.	.	.	.	.	.	.	.	.	.	2	.	.	.	.	.	.	.
EU-8	.	.	.	.	.	.	1	.	.	.	.	.	.	.	.	.	.	.
US-11	.	.	.	.	.	.	.	.	.	.	.	.	.	.	.	.	.	2
US-12	.	1	.	.	.	.	.	.	.	.	.	.	.	.	.	.	.	.
US-14	.	.	.	.	.	1	.	.	.	.	.	.	.	.	.	.	.	.
US-17	.	.	.	.	.	.	.	.	.	.	.	1	.	.	.	.	.	.
US-20	2	.	.	.	.	.	.	.	.	.	.	.	.	.	.	.	.	.
US-21	.	.	.	.	.	.	.	.	.	.	.	.	.	.	.	.	2	.
US-22	.	.	.	.	.	.	.	.	.	.	.	.	2	.	.	.	.	.
US-23	.	.	.	.	.	.	.	3	.	.	.	.	.	.	.	.	.	.
US-24	.	.	.	.	3	.	.	.	.	.	.	.	.	.	.	.	.	.
US-8	.	.	1	1	.	2	.	.	.	.	.	.	.	.	.	.	.	.

FIGURE LEGENDS

294   **Figure 1** Diagrammatic representation of the three clustering algorithms implemented in `mlg.filter`.
295   (**A-C**) Represent different clustering algorithms on the same imaginary network with a threshold of 0.451.
296   Edge weights are represented in arbitrary units noted by the line thickness and numerical values next to
297   the lines. All outer angles are 90 degrees, so the un-labeled edge weights can be obtained with simply
298   geometry. Colored circles represent clusters of genotypes. (**A**) Farthest neighbor clustering does not cluster
299   nodes B and C because nodes A and C are more than a distance of 0.451 apart. (**B**) UPGMA (average
300   neighbor) clustering clusters nodes A, B, and C together because the average distance between them and

301 C is < 0.451. (**C**) Nearest neighbor clustering clusters all nodes together because the minimum distance
302 between them is always < 0.451.

303 **Figure 2** Graphical representation of three different clustering algorithms collapsing multilocus
304 genotypes for 12 SSR loci from *Phytophthora infestans* representing 18 clonal lineages. The horizontal
305 axis is Bruvo's genetic distance assuming the genome addition model. The vertical axis represents the
306 number of multilocus lineages observed. Each point shows the threshold at which one would observe a
307 given number of multilocus genotypes. The horizontal black line represents 18 multilocus genotypes and
308 vertical dashed lines mark the thresholds used to collapse the multilocus genotypes into 18 multilocus
309 lineages.

310 **Figure 3** (**A-B**) Minimum spanning networks of the hemagglutinin (HA) segment of H3N2 viral DNA
311 from the *adegenet* package representing flu epidemics from 2001 to 2006 without reticulation (**A**) and with
312 reticulation (**B**) (Jombart, 2008; Jombart et al., 2010). Each node represents a unique multilocus genotype,
313 colors represent epidemic year, and edge color represents absolute genetic distance. (**C**) Shannon entropy
314 values for population assignments compared with communities determined by the infoMAP algorithm on
315 (**A**) and (**B**). (**D**) Graphic reproduced from Jombart et al. (2010) showing that the 2006 epidemic does not
316 cluster neatly with the other years.

317 **Figure 4** UPGMA dendrogram generated from Nei's genetic distance on 15 breeds of *Bos taurus* (BT)
318 or *Bos indicus* (BI) from Africa (AF) or France (FR). These data are from Laloë et al. (2007). Node labels
319 represent bootstrap support > 50% out of 1,000 bootstrap replicates.

320 **Figure 5** Genotype accumulation curve for 694 isolates of the peach brown rot pathogen, *Monilinia*
321 *fructicola* genotyped over 13 loci from Everhart and Scherm (2015). The horizontal axis represents the
322 number of loci randomly sampled without replacement up to $n-1$ loci, the vertical axis shows the number
323 of multilocus genotypes observed, up to 262, the number of unique multilocus genotypes in the data set.
324 The red dashed line represents 90% of the total observed multilocus genotypes. A trendline (blue) has
325 been added using the *ggplot2* function `stat_smooth`.

326 **Figure 6** (**A**) Sliding window analysis of the standardized index of association ($\bar{r}_d$) across a simulated
327 1.1×10^4 nt chromosome containing 1,100 variants among 100 individuals. Each window analyzed
328 variants within 500nt chunks. The black line refers to the clonal and the blue line to the sexual populations.
329 (**B**) boxplots showing 100 random samples of 50 variants to calculate a distribution of $\bar{r}_d$ for the clonal
330 (red) and sexual (blue) populations. Each box is centered around the mean, with whiskers extending out
331 to 1.5 times the interquartile range. The median is indicated by the center line. (**A**) and (**B**) are plotted on
332 the same y-axis.

REFERENCES

333 Agapow, P.-M., and Burt, A. (2001). Indices of multilocus linkage disequilibrium. *Molecular Ecology*
334 *Notes* 1, 101–102. doi:10.1046/j.1471-8278.2000.00014.x.

335 Anderson, J. B., and Kohn, L. M. (1995). Clonality in soilborne, plant-pathogenic fungi. *Annual review*
336 *of phytopathology* 33, 369–391.

337 Arnaud-Hanod, S., Duarte, C. M., Alberto, F., and Serrão, E. A. (2007). Standardizing methods to
338 address clonality in population studies. *Molecular Ecology* 16, 5115–5139.

339 Brown, A., Feldman, M., and Nevo, E. (1980). Multilocus structure of natural populations of *Hordeum*
340 *spontaneum*. *Genetics* 96, 523–536. Available at: `http://www.genetics.org/content/96/2/`
341 `523.abstract`.

342 Bruvo, R., Michiels, N. K., D'Souza, T. G., and Schulenburg, H. (2004). A simple method for the
343 calculation of microsatellite genotype distances irrespective of ploidy level. *Molecular Ecology* 13, 2101–
344 2106.

345 Chakarov, N., Linke, B., Boerner, M., Goesmann, A., Krüger, O., and Hoffman, J. I. (2015). Apparent
346 vector-mediated parent-to-offspring transmission in an avian malaria-like parasite. *Molecular ecology* 24,
347 1355–1363.

348 Cooke, D. E., Cano, L. M., Raffaele, S., Bain, R. A., Cooke, L. R., Etherington, G. J., Deahl, K. L.,
349 Farrer, R. A., Gilroy, E. M., Goss, E. M., et al. (2012). Genome analyses of an aggressive and invasive
350 lineage of the Irish potato famine pathogen. *PLoS pathogens* 8, e1002940.

351 Csardi, G., and Nepusz, T. (2006). The igraph software package for complex network research.
352 *InterJournal* Complex Systems, 1695. Available at: `http://igraph.org`.

353 Dagum, L., and Menon, R. (1998). OpenMP: An industry standard API for shared-memory
354 programming. *Computational Science & Engineering, IEEE* 5, 46–55.

355 Davey, J. W., and Blaxter, M. L. (2010). RADSeq: Next-generation population genetics. *Briefings in
356 Functional Genomics* 9, 416–423. doi:10.1093/bfgp/elq031.

357 Davey, J. W., Hohenlohe, P. A., Etter, P. D., Boone, J. Q., Catchen, J. M., and Blaxter, M. L.
358 (2011). Genome-wide genetic marker discovery and genotyping using next-generation sequencing. *Nature
359 Reviews Genetics* 12, 499–510.

360 Dobzhansky, T. (1973). Nothing in biology makes sense except in the light of evolution. *The American
361 Biology Teacher* 75, 87–91.

362 Elshire, R. J., Glaubitz, J. C., Sun, Q., Poland, J. A., Kawamoto, K., Buckler, E. S., and Mitchell, S. E.
363 (2011). A robust, simple genotyping-by-sequencing (GBS) approach for high diversity species. *PloS one*
364 6, e19379.

365 Everhart, S., and Scherm, H. (2015). Fine-scale genetic structure of *Monilinia fructicola* during brown
366 rot epidemics within individual peach tree canopies. *Phytopathology* 105, 542–549.

367 Excoffier, L., Smouse, P. E., and Quattro, J. M. (1992). Analysis of molecular variance inferred from
368 metric distances among DNA haplotypes: Application to human mitochondrial DNA restriction data.
369 *Genetics* 131, 479–491.

370 Falush, D., Stephens, M., and Pritchard, J. K. (2003). Inference of population structure using multilocus
371 genotype data: Linked loci and correlated allele frequencies. *Genetics* 164, 1567–1587. Available at:
372 `http://www.genetics.org/content/164/4/1567.abstract`.

373 Goss, E. M., Larsen, M., Chastagner, G. A., Givens, D. R., and Grünwald, N. J. (2009). Population
374 genetic analysis infers migration pathways of *Phytophthora ramorum* in US nurseries. *PLoS pathogens* 5,
375 e1000583.

376 Goss, E. M., Tabima, J. F., Cooke, D. E., Restrepo, S., Fry, W. E., Forbes, G. A., Fieland, V. J., Cardenas,
377 M., and Grünwald, N. J. (2014). The Irish potato famine pathogen *Phytophthora infestans* originated in
378 central Mexico rather than the Andes. *Proceedings of the National Academy of Sciences* 111, 8791–8796.

379 Goudet, J. (2005). Hierfstat, a package for R to compute and test hierarchical F-statistics. *Molecular
380 Ecology Notes* 5, 184–186.

381 Gross, A., Hosoya, T., and Queloz, V. (2014). Population structure of the invasive forest pathogen
382 *Hymenoscyphus pseudoalbidus*. *Molecular ecology* 23, 2943–2960.

383 Grünwald, N. J., and Goss, E. M. (2011). Evolution and population genetics of exotic and re-emerging
384 pathogens: Novel tools and approaches. *Annual Review of Phytopathology* 49, 249–267.

385 Grünwald, N. J., and Hoheisel, G.-A. (2006). Hierarchical analysis of diversity, selfing, and genetic
386 differentiation in populations of the oomycete *Aphanomyces euteiches*. *Phytopathology* 96, 1134–1141.

387 Grünwald, N. J., Goodwin, S. B., Milgroom, M. G., and Fry, W. E. (2003). Analysis of genotypic
388 diversity data for populations of microorganisms. *Phytopathology* 93, 738–46. Available at: `http://`
389 `apsjournals.apsnet.org/doi/abs/10.1094/PHYTO.2003.93.6.738`.

390 Grünwald, N. J., Martin, F. N., Larsen, M. M., Sullivan, C. M., Press, C. M., Coffey, M. D., Hansen,
391 E. M., and Parke, J. L. (2011). Phytophthora-iD. org: A sequence-based phytophthora identification tool.
392 *Plant Disease* 95, 337–342.

393 Jombart, T. (2008). Adegenet: a R package for the multivariate analysis of genetic markers.
394 *Bioinformatics* 24, 1403–1405. doi:10.1093/bioinformatics/btn129.

395 Jombart, T., and Ahmed, I. (2011). Adegenet 1.3-1: New tools for the analysis of genome-wide SNP
396 data. *Bioinformatics* 27, 3070–3071.

397 Jombart, T., Devillard, S., and Balloux, F. (2010). Discriminant analysis of principal components: A
398 new method for the analysis of genetically structured populations. *BMC genetics* 11, 94.

399 Kamvar, Z. N., Larsen, M. M., Kanaskie, A. M., Hansen, E. M., and Grünwald, N. J. (2015). Spatial and
400 temporal analysis of populations of the sudden oak death pathogen in Oregon forests. *Phytopathology*, in
401 press.

402 Kamvar, Z. N., Larsen, M. M., Kanaskie, A. M., Hansen, E. M., and Grünwald, N. J. (2014a).
403 Sudden_Oak_Death_in_Oregon_Forests: Spatial and temporal population dynamics of the sudden oak
404 death epidemic in Oregon Forests. doi:10.5281/zenodo.13007.

405 Kamvar, Z. N., Tabima, J. F., and Grünwald, N. J. (2014b). Poppr: An R package for genetic analysis of
406 populations with clonal, partially clonal, and/or sexual reproduction. *PeerJ* 2, e281.

407 Laloë, D., Jombart, T., Dufour, A.-B., and Moazami-Goudarzi, K. (2007). Consensus genetic structuring
408 and typological value of markers using multiple co-inertia analysis. *Genetics Selection Evolution* 39, 1–23.

409 Lees, A., Wattier, R., Shaw, D., Sullivan, L., Williams, N., and Cooke, D. (2006). Novel microsatellite
410 markers for the analysis of *Phytophthora infestans* populations. *Plant Pathology* 55, 311–319.

411 Li, Y., Cooke, D. E., Jacobsen, E., and Lee, T. van der (2013). Efficient multiplex simple sequence repeat
412 genotyping of the oomycete plant pathogen *Phytophthora infestans*. *Journal of microbiological methods*
413 92, 316–322.

414 Linde, C., Zhan, J., and McDonald, B. (2002). Population structure of *Mycosphaerella graminicola*:
415 From lesions to continents. *Phytopathology* 92, 946–955.

416 Luikart, G., England, P. R., Tallmon, D., Jordan, S., and Taberlet, P. (2003). The power and promise of
417 population genomics: From genotyping to genome typing. *Nature Reviews Genetics* 4, 981–994.

418 Mantel, N. (1967). The detection of disease clustering and a generalized regression approach. *Cancer*
419 *research* 27, 209–220.

420 Mastretta-Yanes, A., Arrigo, N., Alvarez, N., Jorgensen, T. H., Piñero, D., and Emerson, B.
421 (2015). Restriction site-associated DNA sequencing, genotyping error estimation and de novo assembly
422 optimization for population genetic inference. *Molecular ecology resources* 15, 28–41.

423 McDonald, B. A., and Linde, C. (2002). The population genetics of plant pathogens and breeding
424 strategies for durable resistance. *Euphytica* 124, 163–180. doi:10.1023/A:1015678432355.

425 Meirmans, P. G., and Van Tienderen, P. H. (2004). GENOTYPE and GENODIVE: Two programs for
426 the analysis of genetic diversity of asexual organisms. *Molecular Ecology Notes* 4, 792–794.

427 Metzger, M. J., Reinisch, C., Sherry, J., and Goff, S. P. (2015). Horizontal transmission of clonal cancer
428 cells causes leukemia in soft-shell clams. *Cell* 161, 255–263.

429 Michalakis, Y., and Excoffier, L. (1996). A generic estimation of population subdivision using distances
430 between alleles with special reference for microsatellite loci. *Genetics* 142, 1061–1064.

431 Milgroom, M. G. (1996). Recombination and the multilocus structure of fungal populations. *Annual*
432 *review of phytopathology* 34, 457–477.

433 Milgroom, M. G., Levin, S. A., and Fry, W. E. (1989). Population genetics theory and fungicide
434 resistance. *Plant disease epidemiology* 2, 340–367.

435 Nei, M. (1973). Analysis of gene diversity in subdivided populations. *Proceedings of the National*
436 *Academy of Sciences* 70, 3321–3323.

437 Oksanen, J., Blanchet, F. G., Kindt, R., Legendre, P., Minchin, P. R., O'Hara, R. B., Simpson, G. L.,
438 Solymos, P., Stevens, M. H. H., and Wagner, H. (2015). *Vegan: Community ecology package*. Available
439 at: `http://CRAN.R-project.org/package=vegan`.

440 Paradis, E. (2010). Pegas: an R package for population genetics with an integrated–modular approach.
441 *Bioinformatics* 26, 419–420.

442 Prevosti, A., Ocaña, J., and Alonso, G. (1975). Distances between populations of *Drosophila*
443 *subobscura*, based on chromosome arrangement frequencies. *Theoretical and Applied Genetics* 45,
444 231–241.

445 R Core Team (2015). *R: A language and environment for statistical computing*. Vienna, Austria: R
446 Foundation for Statistical Computing Available at: `http://www.R-project.org/`.

447 Rosvall, M., and Bergstrom, C. T. (2008). Maps of random walks on complex networks reveal
448 community structure. *Proceedings of the National Academy of Sciences* 105, 1118–1123.

449 Shannon, C. (2001). A mathematical theory of communication. *ACM SIGMOBILE Mobile Computing*
450 *and Communications Review* 5, 3–55. Available at: `http://cm.bell-labs.com/cm/ms/what/`
451 `shannonday/shannon1948.pdf`.

452 Smith, J. M., Smith, N. H., O'Rourke, M., and Spratt, B. G. (1993). How clonal are bacteria?
453 *Proceedings of the National Academy of Sciences* 90, 4384–4388. doi:10.1073/pnas.90.10.4384.

454 Sokal, R. R. (1958). A statistical method for evaluating systematic relationships. *Univ Kans Sci Bull* 38,
455 1409–1438.

456 Taylor, J. W., and Fisher, M. C. (2003). Fungal multilocus sequence typing — it's not just for bacteria.
457 *Current opinion in microbiology* 6, 351–356.

458 Wickham, H., and Chang, W. (2015). *Devtools: Tools to make developing R packages easier*. Available
459 at: `http://CRAN.R-project.org/package=devtools`.

460 Yoshida, K., Schuenemann, V. J., Cano, L. M., Pais, M., Mishra, B., Sharma, R., Lanz, C., Martin,
461 F. N., Kamoun, S., Krause, J., et al. (2013). The rise and fall of the phytophthora infestans lineage that
462 triggered the irish potato famine. *Elife* 2, e00731.